



Cite this: *Chem. Commun.*, 2018, 54, 12990

Received 11th October 2018,  
 Accepted 24th October 2018

DOI: 10.1039/c8cc08168a

rsc.li/chemcomm

## Facile surface functionalization of upconversion nanoparticles with phosphoryl pillar[5]arenes for controlled cargo release and cell imaging†

Xu Wang,<sup>a</sup> Jie Yang,<sup>a</sup> Xiujuan Sun,<sup>b</sup> Hongliang Yu,<sup>a</sup> Fei Yan,<sup>a</sup> Kamel Meguellati,<sup>a</sup> Ziyong Cheng,<sup>c</sup> Haiyuan Zhang<sup>b</sup> and Ying-Wei Yang<sup>\*a</sup>

**Upon surface functionalization and stabilization of  $\beta$ -NaYF<sub>4</sub>:Yb/Er upconversion nanoparticles (UCNPs) with phosphoryl pillar[5]arenes (PP5) via a facile ligand exchange method, we constructed a new hybrid material (PP5-UCNPs) with good water dispersibility especially in a physiological environment and superior capability of controlled cargo release and cell imaging.**

Rare-earth upconversion nanoparticles (UCNPs) are lanthanide ion-doped nanophosphors,<sup>1</sup> holding great promise in lots of technological applications including photocatalysis,<sup>2</sup> bioimaging,<sup>3</sup> and fluorescent bioprobes<sup>4</sup> by virtue of their excellent optical properties. Compared with conventional organic fluorescent dyes and semiconductor quantum dots, UCNPs have distinct photochemical advantages, for instance, thermal and optical stability, low toxicity, large anti-Stokes shifts, sharp emission bands (<10 nm), long luminescence lifetime (micro- to millisecond range), high quantum yields, deep light penetration depths in tissues and minimal auto-fluorescence (background noise).<sup>5</sup> More importantly, UCNPs can convert near-infrared (NIR) light to visible light via sequential electronic excitation and energy transfer processes.<sup>6</sup> And the utilization of NIR excitation enables less damage and deeper penetration into body tissues as compared with UV light, making UCNPs highly suitable for applications in medical diagnosis and treatment, such as *in vivo* imaging and photodynamic therapy.<sup>7,8</sup> Preparation of a water-dispersible and colloiddally stable suspension of UCNPs while retaining their high upconversion efficiencies for biological research is still very challenging.<sup>9</sup> High quality hexagonal-phase UCNPs are commonly prepared in a high-boiling

non-aqueous organic solvent (*e.g.*, 1-octadecene) containing oleic acid (OA) as a coordinating ligand. Meanwhile, the highly luminescent nanoparticles that are coated with OA molecules on the surfaces are incapable of being dispersed in water. Generally, there are several strategies to render the UCNPs dispersible in biological media in the literature.<sup>10</sup> By comparison, the transformation or encapsulation of these nanoparticles by replacing the OA layer with hydrophilic ligands as surfactant-like surface ligands is a better and easier approach.<sup>11</sup>

On the other hand, the design and synthesis of pillar[*n*]arenes (pillarenes) and their derivatives have aroused much attention due to their highly tunable functionality and versatile host-guest properties.<sup>12</sup> Since first reported in 2008,<sup>13</sup> pillarenes have been widely investigated and applied to the fields of drug delivery,<sup>14</sup> molecular machinery,<sup>15</sup> supramolecular polymers,<sup>16</sup> hybrid nanomaterials<sup>17</sup> and so on.<sup>18</sup> It is worth noting that the synthesis of water-soluble pillarenes like phosphatepillar[5,6]arene<sup>19</sup> and other cationic/anionic pillar[5,6]arenes<sup>20</sup> extends the scope of the applications in aqueous or biologically relevant environments. Recently, some attempts on introducing macrocyclic compounds into the system of UCNPs have been made and reported.<sup>21</sup> However, the strategy of combining the advantages of pillarenes and UCNPs has been very rarely investigated,<sup>22</sup> especially, no report is available in the literature to show that pillarenes could be directly used as ligands to modify UCNPs for oral drug delivery system (DDS) applications.

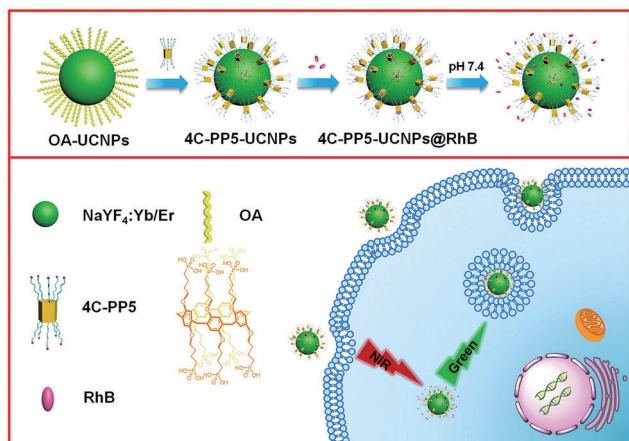
Herein, we report a new pH-responsive DDS based on phosphoryl-functionalized pillar[5]arene (PP5) modified UCNPs for controlled cargo release and cell imaging (Scheme 1). To obtain nanoparticles that are colloiddally stable, we firstly synthesized two kinds of PP5 (2C-PP5/4C-PP5) with different lengths of alkyl groups containing five phosphoryl groups on each rim of the cavity with good water dispersibility (Schemes S1 and S2, ESI†) and then decorated them, respectively, onto the surfaces of  $\beta$ -NaYF<sub>4</sub>:Yb/Er nanoparticles (OA-UCNPs) via a ligand-exchange method to get the PP5-stabilized UCNPs, namely, 2C-PP5-UCNPs and 4C-PP5-UCNPs. Considering the similar properties of 2C-PP5-UCNPs and 4C-PP5-UCNPs, 4C-PP5 is easier to obtain

<sup>a</sup> State Key Laboratory of Inorganic Synthesis and Preparative Chemistry, International Joint Research Laboratory of Nano-Micro Architecture Chemistry (NMAC), College of Chemistry, Jilin University, 2699 Qianjin Street, Changchun 130012, P. R. China. E-mail: ywyang@jlu.edu.cn

<sup>b</sup> Laboratory of Chemical Biology, Changchun Institute of Applied Chemistry, Chinese Academy of Sciences, Changchun 130022, P. R. China

<sup>c</sup> State Key Laboratory of Rare Earth Resource Utilization, Changchun Institute of Applied Chemistry, Chinese Academy of Sciences, Changchun 130022, P. R. China

† Electronic supplementary information (ESI) available. See DOI: 10.1039/c8cc08168a



**Scheme 1** Schematic representation of the construction of 4C-PP5-UCNPs@RhB nanosystem and its application for targeted drug delivery and UCL cell imaging.

in relatively high yield than 2C-PP5, and we selected 4C-PP5-UCNPs for the subsequent experiments. As a proof-of-concept, rhodamine B (RhB) was employed as a kind of drug model for loading into the nanomaterials *via* host-guest and electrostatic interactions, leading to the formation of a special pH-responsive controlled release nanosystem, *i.e.*, 4C-PP5-UCNPs@RhB. Meanwhile, macrophages were chosen to explore the biocompatibility and upconversion luminescence (UCL) cell imaging under NIR irradiation of this nanosystem. To our satisfaction, 4C-PP5-UCNPs were proven to be a promising candidate for therapeutics combining controlled cargo release and cell imaging.

To confirm the successful ligand-exchange of OA on the UCNP surface by 4C-PP5, a series of investigations were performed (Fig. 1 and 2). As shown in the TEM and SEM images (Fig. 1a and c), the synthesized monodisperse OA-UCNPs show a hexagonal phase. Compared to OA-UCNPs, 4C-PP5-UCNPs have no obvious changes in the size and morphology. The TEM and SEM images (Fig. 1b and d) of 4C-PP5-UCNPs show good dispersibility in water and the average particle size is around  $31.4 \pm 4.2$  nm (Fig. S1, ESI<sup>†</sup>), which demonstrated that the 4C-PP5 ligands are capable of effectively stabilizing the UCNPs in water. Elemental mapping of 4C-PP5-UCNPs further provided

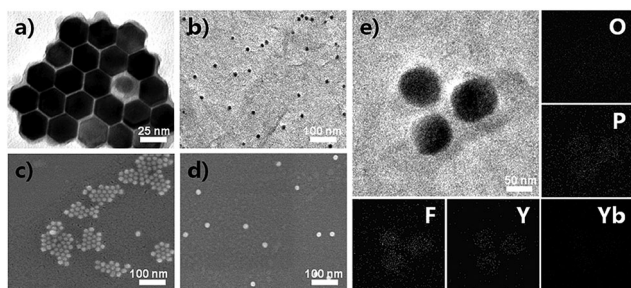


**Fig. 1** TEM images of (a) OA-UCNPs and (b) 4C-PP5-UCNPs; SEM images of (c) OA-UCNPs and (d) 4C-PP5-UCNPs; (e) elemental mapping of 4C-PP5-UCNPs.

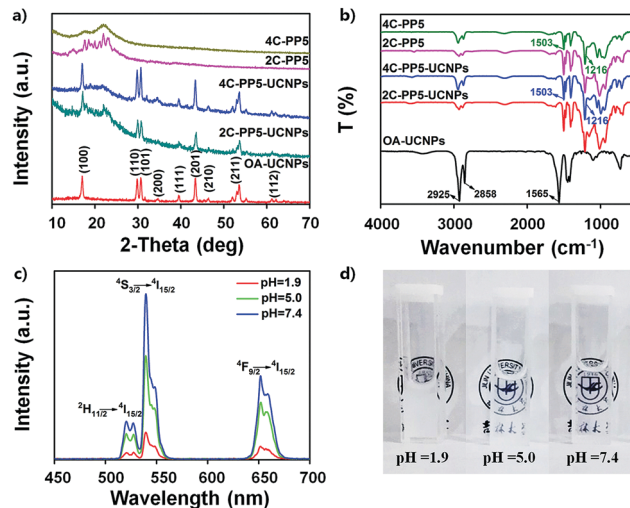


**Fig. 2** (a) PXRD patterns and (b) FT-IR spectra of OA-UCNPs, 2C-PP5-UCNPs, 4C-PP5-UCNPs, 2C-PP5, and 4C-PP5; (c) upconversion emission spectra and (d) stability images of 4C-PP5-UCNPs in PBS.

convincing evidence that the UCNPs were coated with phosphor-containing 4C-PP5 macrocycles (Fig. 1e).

The successful preparation of 2C-PP5-UCNPs and 4C-PP5-UCNPs was further verified by powder X-ray diffraction (PXRD), Fourier transform infrared (FT-IR) spectroscopy, and upconversion emission spectroscopy (Fig. 2). The PXRD pattern (Fig. 2a) of OA-UCNPs exhibits peak positions and intensities that can be well indexed in accord with hexagonal-phase  $\beta$ - $\text{NaYF}_4$  crystals, which is in good agreement with the data reported in the JCPDS standard card (28-1192). After the ligand-exchange, 2C-PP5-UCNPs and 4C-PP5-UCNPs show almost the same peak patterns as OA-UCNPs. In addition, PXRD results suggest the high crystallinity of the resulting UCNPs from ligand exchange. FT-IR characterization was employed to confirm the presence of pillarene macrocycles on the surface of ligand-exchanged UCNPs (Fig. 2b).<sup>22</sup> The as-prepared OA-UCNPs exhibit the carboxylate anion absorption peaks at  $1565$  and  $1485$   $\text{cm}^{-1}$ , and the peaks at  $2858$  and  $2925$   $\text{cm}^{-1}$  could be assigned to the asymmetric and symmetric stretching vibrations of  $\text{CH}_2$  in the alkyl chains.<sup>23</sup> The FT-IR spectra of the two pillarene-exchanged UCNPs did not show any carboxylate anion peaks coming from the octadecyl of oleic acid, but instead clearly showed peaks corresponding to the phosphoryl coordination ( $\nu_{\text{P-O}} = 1050$   $\text{cm}^{-1}$ ,  $\nu_{\text{P=O}} = 1216$   $\text{cm}^{-1}$ ) and the vibration  $\beta_{\text{Ar-H}}$  of the benzene ( $1503$   $\text{cm}^{-1}$ ). The characteristic peak at  $1503$   $\text{cm}^{-1}$  attributing to the band vibration  $\beta_{\text{Ar-H}}$  of the benzene could also be found in the pure 2C-PP5 and 4C-PP5 samples. Apparently, the OA molecules have been replaced by the pillarene ligands. To further verify the ligand-exchange method, the monomer 1,4-(phosphonic acid)butoxybenzene (M3) was used as a control to prepare M3-stabilized UCNPs (M3-UCNPs). The results show that M3-UCNPs with regular morphology are prepared successfully and dispersed well in water (Fig. S2 and S3, ESI<sup>†</sup>). Thus, we can conclude that phosphoryl plays a crucial role in the ligand-exchange process.

Characteristic violet, green, and red upconversion emissions of the  $\text{Er}^{3+}$ -based UCNPs, corresponding to the  ${}^2\text{H}_{11/2} \rightarrow {}^4\text{I}_{15/2}$ ,  ${}^4\text{S}_{3/2} \rightarrow {}^4\text{I}_{15/2}$ , and  ${}^4\text{F}_{9/2} \rightarrow {}^4\text{I}_{15/2}$  transitions, respectively, are shown in Fig. 2c. Water solubility or dispersibility of UCNPs is a very essential element for their bio-applications. We investigated the degree of water stability of the 4C-PP5-UCNPs in phosphate-buffered saline (PBS) at different pH values (Fig. 2d). Aggregation and turbidity occur under more acidic conditions. With the increase of the pH value, the aggregation gradually becomes dispersible in aqueous media. At pH 7.4, the dispersion becomes a clear solution. This could be attributed to the deprotonation of phosphoryl groups of the 4C-PP5 macrocycle, leading to a better water-solubility of the final nanoparticles.

5-Aminosalicylic acid (5-ASA), one of the most commonly used anti-inflammatory drugs, was loaded in the 4C-PP5-UCNPs (4C-PP5-UCNPs@5-ASA) in its hydrochloride salt form *via* a similar method to the loading of RhB. Dynamic light scattering (DLS) study shows the hydrous particle diameters of 4C-PP5-UCNPs, 4C-PP5-UCNPs@RhB, and 4C-PP5-UCNPs@5-ASA as 38, 44 and 43 nm in PBS (pH 7.4), respectively (Fig. S4de and f, ESI<sup>†</sup>). The zeta potentials of 4C-PP5-UCNPs before and after RhB/5-ASA loading changed from  $-48.5$  to  $-30.0$  and  $-34.4$  mV, respectively, indicating the successful cargo loading (Fig. S5, ESI<sup>†</sup>). Thermogravimetric (TGA) analysis of 4C-PP5-UCNPs shows a mass loss of 49.6% that is attributed to the mass of 4C-PP5 on the UCNPs (Fig. S6, ESI<sup>†</sup>). The losses of 3.4% and 4.1% in 4C-PP5-UCNPs@RhB and 4C-PP5-UCNPs@5-ASA, respectively, represent the masses of the RhB and 5-ASA loaded in the systems.

The controlled release of RhB from 4C-PP5-UCNPs@RhB was monitored by using UV-vis spectroscopy. We know that the stomach (pH 1.9) is in acidic conditions and the pH environment of the small bowel, colon and rectum is relatively higher (pH 5.5–7.4).<sup>24</sup> To use an oral medicine for targeted treatment of inflammatory bowel disease (IBD), the development and utilization of an effective pH-responsive oral DDS is of great importance.<sup>25</sup> As a proof-of-concept-study, we simulated the different pH environments of the gastrointestinal tract to study the release process of a RhB cargo, which include pH 1.9 (stomach), 5.0 (small intestine) and 7.4 (colon), respectively (Fig. 3). The amount of RhB released from 4C-PP5-UCNPs@RhB reached 72% within 90 min at pH 7.4, while less than 17% and 2% within the same period of time at pH 5.0 and 1.9, respectively (Fig. 3a). Then, we placed 4C-PP5-UCNPs@RhB in the

solution of pH 1.9 for 2 h, pH 5.0 for 1 h, and pH 7.4 for 7 h in turn (Fig. 3b), which clearly showed the good pH responsiveness of this DDS. All of these results indicated the RhB release efficiency of the materials upon increasing the solution pH. When the pH value is higher than the  $\text{pK}_a$  of RhB (3.7), the cationic form of the carboxyl group of RhB ( $\text{RhB}^+$ ) is deprotonated and transformed into the zwitterionic form ( $\text{RhB}^\pm$ ).<sup>26</sup> Phosphonic acids have two protons that can be dissociated under different conditions ( $\text{pK}_{a1} \sim 2.4$ ;  $\text{pK}_{a2} \sim 8.0$ ) (Fig. S7, ESI<sup>†</sup>).<sup>27</sup> At pH 1.9, the host-guest interaction plays a leading role between PP5 and RhB. While at pH 5.0–7.4, the phosphonates of PP5 preferentially carried single negative charges. Upon increasing the pH, the phosphate groups of PP5 were further deprotonated, resulting in the strengthening of the electrostatic repulsion between the negatively charged PP5 and the negatively charged  $\text{COO}^-$  group of RhB. To quantitatively measure the binding of RhB and 5-ASA with PP5, fluorescence titrations were performed at 298 K in PBS (pH 5.0 and 7.4). At pH 5.0, the association constants ( $K_a$ ) of 4C-PP5 with RhB and 5-ASA were calculated to be  $(2.7 \pm 0.3) \times 10^5 \text{ M}^{-1}$  and  $(4.2 \pm 0.7) \times 10^5 \text{ M}^{-1}$ , respectively (Fig. S8 and S10, ESI<sup>†</sup>). Meanwhile, the  $K_a$  values were calculated to be  $(1.3 \pm 0.5) \times 10^5 \text{ M}^{-1}$  and  $(1.3 \pm 0.1) \times 10^4 \text{ M}^{-1}$  for RhB and 5-ASA at pH 7.4, respectively (Fig. S9 and S11, ESI<sup>†</sup>) and these  $K_a$  values were smaller than the  $K_a$  values at pH 5.0.

To evaluate the biocompatibility of this nanosystem, *in vitro* cell viability studies of 4C-PP5-UCNPs were carried out *via* the 3-(4',5'-dimethylthiazol-2'-yl)-2,5-diphenyl tetrazolium bromide (MTT) assay on macrophages and L02 cells (Fig. 4a and b), respectively. Compared with the control group, the cell viabilities of 4C-PP5-UCNP groups were more than 85% both on macrophages and L02 cells even at a high concentration of  $125 \mu\text{g mL}^{-1}$ , indicating that 4C-PP5-UCNPs had good biocompatibility and are promising for application in biological systems. It is always a research hotspot to use UCNPs for cell imaging owing to their excellent upconversion fluorescence properties. Thus, macrophages were chosen to investigate the UCL cell imaging of 4C-PP5-UCNPs, 4C-PP5-UCNPs@RhB and 4C-PP5-UCNPs@5-ASA. As shown in Fig. 4c, all these three kinds of nanoparticles can be taken up to the cytoplasm and emit bright green light under the excitation of a 980 nm laser. Among them, more 4C-PP5-UCNPs@RhB and 4C-PP5-UCNPs@5-ASA nanoparticles were taken up to the cells under the same conditions, which was mainly on account of the zeta potential of 4C-PP5-UCNPs after cargo loading increasing and becoming closer to the zeta potential of cytomembrane. Above all, because of the good biocompatibility and upconversion fluorescence properties, 4C-PP5-UCNPs could be a desirable candidate for high-contrast intracellular fluorescence imaging.

In summary, an efficient and feasible strategy for the synthesis of water-dispersible UCNPs, which can form stable and transparent solutions in a physiological environment, has been established *via* surface-ligand exchange of oleate with phosphoryl pillarenes. These nanoparticles were further used for the successful preparation of a pH-responsive DDS *via* the host-guest and electrostatic interactions between PP5 and cargoes. The release efficiency of a drug or a model drug from this

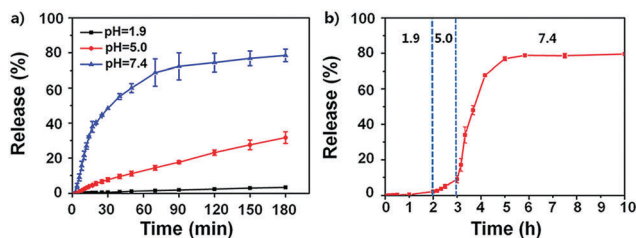


Fig. 3 (a) Release profiles of RhB from 4C-PP5-UCNPs@RhB in PBS; (b) release profiles of RhB from 4C-PP5-UCNPs@RhB under the simulated variable pH conditions of transit through the gastrointestinal tract.

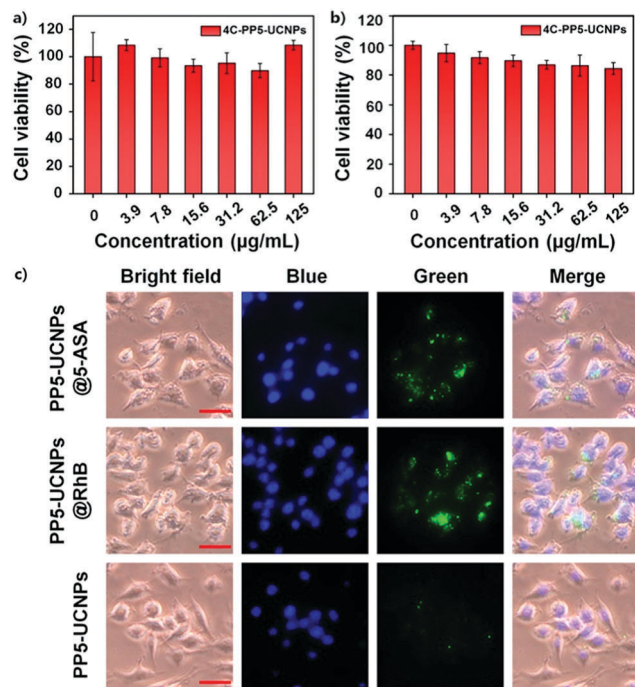


Fig. 4 Cytotoxicity assay of (a) macrophages and (b) L02 cells in the presence of 4C-PP5-UCNPs; (c) the bright and fluorescence microscopy images of macrophages incubated with  $100 \mu\text{g mL}^{-1}$  of 4C-PP5-UCNPs, 4C-PP5-UCNPs@RhB and 4C-PP5-UCNPs@5-ASA for 6 h, respectively. 4C-PP5-UCNPs inside cells were excited by a 980 nm wavelength laser as the light source. Each series can be classified into the bright field image, the nuclei of macrophages, the UCL image and the merging of the first three images, respectively. Scale bar:  $10 \mu\text{m}$ .

system increases with the increase of the environment pH values. Interestingly, this nanosystem could also realize UCL cell imaging under NIR irradiation. This research provides an insight into the development of phosphorylpillarene-coated UCNPs for improved treatment of IBD.

We thank the National Natural Science Foundation of China (51673084, 51473061, and 21871108), the Jilin Province-University Cooperative Construction Project—Special Funds for New Materials (SXGJSF2017-3), and the Jilin University Talents Cultivation Program for financial support.

## Conflicts of interest

There are no conflicts to declare.

## Notes and references

- G. Bai, M.-K. Tsang and J. Hao, *Adv. Funct. Mater.*, 2016, **26**, 6330–6350.
- D. Li, S.-H. Yu and H.-L. Jiang, *Adv. Mater.*, 2018, **30**, 1707377.
- W. Zheng, P. Huang, D. Tu, E. Ma, H. Zhu and X. Chen, *Chem. Soc. Rev.*, 2015, **44**, 1379–1415.
- X. Li, F. Zhang and D. Zhao, *Chem. Soc. Rev.*, 2015, **44**, 1346–1378.
- R. Wei, Z. Wei, L. Sun, J. Z. Zhang, J. Liu, X. Ge and L. Shi, *ACS Appl. Mater. Interfaces*, 2016, **8**, 400–410.

- S. Chen, A. Z. Weitemier, X. Zeng, L. He, X. Wang, Y. Tao, A. J. Y. Huang, Y. Hashimoto, M. Kano, H. Iwasaki, L. K. Parajuli, S. Okabe, D. B. L. Teh, A. H. All, I. Tsutsui-Kimura, K. F. Tanaka, X. Liu and T. J. McHugh, *Science*, 2018, **359**, 679–684.
- J. Rieffel, F. Chen, J. Kim, G. Chen, W. Shao, S. Shao, U. Chitgupi, R. Hernandez, S. A. Graves, R. J. Nickles, P. N. Prasad, C. Kim, W. Cai and J. F. Lovell, *Adv. Mater.*, 2015, **27**, 1785–1790.
- J. Xu, P. Yang, M. Sun, H. Bi, B. Liu, D. Yang, S. Gai, F. He and J. Lin, *ACS Nano*, 2017, **11**, 4133–4144.
- J. Liu, A. M. Kaczmarek, J. Billet, I. V. Driesscheb and R. V. Deun, *Dalton Trans.*, 2016, **45**, 12094–12102.
- Z. Gu, L. Yan, G. Tian, S. Li, Z. Chai and Y. Zhao, *Adv. Mater.*, 2013, **25**, 3758–3779.
- J.-C. Boyer, M.-P. Manseau, J. I. Murray and F. C. J. M. Veggel, *Langmuir*, 2010, **26**, 1157–1164.
- (a) T. Ogoshi, Y. Shimada, Y. Sakata, S. Akine and T. Yamagishi, *J. Am. Chem. Soc.*, 2017, **139**, 5664–5667; (b) N. Song, T. Kakuta, T. Yamagishi, Y.-W. Yang and T. Ogoshi, *Chem*, 2018, **4**, 2029–2053.
- T. Ogoshi, S. Kanai, S.-H. Fujinami, T. Yamagishi and Y. Nakamoto, *J. Am. Chem. Soc.*, 2008, **130**, 5022–5023.
- (a) Q. Hao, Y. Chen, Z. Huang, J.-F. Xu, Z. Sun and X. Zhang, *ACS Appl. Mater. Interfaces*, 2018, **10**, 5365–5372; (b) N. Song and Y.-W. Yang, *Chem. Soc. Rev.*, 2015, **44**, 3474–3504.
- X.-S. Du, C.-Y. Wang, Q. Jia, R. Deng, H.-S. Tian, H.-Y. Zhang, K. Meguellati and Y.-W. Yang, *Chem. Commun.*, 2017, **53**, 5326–5329.
- (a) Y. Wang, M.-Z. Lv, N. Song, Z.-J. Liu, C.-Y. Wang and Y.-W. Yang, *Macromolecules*, 2017, **50**, 5759–5766; (b) X.-Y. Lou and Y.-W. Yang, *Adv. Opt. Mater.*, 2018, **6**, 1800668.
- (a) M.-X. Wu, J. Gao, F. Wang, J. Yang, N. Song, X. Jin, P. Mi, J. Tian, J. Luo, F. Liang and Y.-W. Yang, *Small*, 2018, **14**, 1704440; (b) M.-X. Wu, H.-J. Yan, J. Gao, Y. Cheng, J. Yang, J.-R. Wu, B.-J. Gong, H. Zhang and Y.-W. Yang, *ACS Appl. Mater. Interfaces*, 2018, **10**, 34655–34663; (c) Q.-L. Li, Y. Sun, L. Ren, X. Wang, C. Wang, L. Li, Y.-W. Yang, X. Yu and J. Yu, *ACS Appl. Mater. Interfaces*, 2018, **10**, 29314–29324.
- (a) J.-R. Wu, A. Mu, B. Li, C.-Y. Wang, L. Fang and Y.-W. Yang, *Angew. Chem., Int. Ed.*, 2018, **57**, 9853–9858; (b) J.-R. Wu, C.-Y. Wang, Y. Tao, Y. Wang, C. Li and Y.-W. Yang, *Eur. J. Org. Chem.*, 2018, 1321–1325; (c) B. Gao, L.-L. Tan, N. Song, K. Li and Y.-W. Yang, *Chem. Commun.*, 2016, **52**, 5804–5807; (d) X. Li, Z. Li and Y.-W. Yang, *Adv. Mater.*, 2018, **30**, 1800177; (e) L.-L. Tan, Y. Zhu, Y. Jin, W. Zhang and Y.-W. Yang, *Supramol. Chem.*, 2018, **30**, 648–654.
- (a) X. Huang, S. Wu, X. Ke, X. Li and X. Du, *ACS Appl. Mater. Interfaces*, 2017, **9**, 19638–19645; (b) W. Cheng, H. Tang, R. Wang, L. Wang, H. Meier and D. Cao, *Chem. Commun.*, 2016, **52**, 8075–8078.
- Y. Zhou, K. Jie and F. Huang, *Org. Chem. Front.*, 2017, **4**, 2387–2391.
- (a) L. Francés-Soriano, S. González-Carrero, E. Navarro-Raga, R. E. Galian, M. González-Béjar and J. Pérez-Prieto, *Adv. Funct. Mater.*, 2016, **26**, 5131–5138; (b) B. Gu, Y. Zhou, X. Zhang, X. Liu, Y. Zhang, R. Marks, H. Zhang, X. Liu and Q. Zhang, *Nanoscale*, 2016, **8**, 276–282.
- H. Li, R. Wei, G.-H. Yan, J. Sun, C. Li, H. Wang, L. Shi, J. A. Capobianco and L. Sun, *ACS Appl. Mater. Interfaces*, 2018, **10**, 4910–4920.
- B. Liu, C. Li, B. Xing, P. Yang and J. Lin, *J. Mater. Chem. B*, 2016, **4**, 4884–4894.
- (a) J. M. Gamboa and K. W. Leong, *Adv. Drug Delivery Rev.*, 2013, **65**, 800–810; (b) S. G. Nugent, D. Kumar, D. S. Rampton and D. F. Evans, *Gut*, 2001, **48**, 571–577; (c) E.-Y. Chuang, K.-J. Lin, T.-Y. Huang, H.-L. Chen, Y.-B. Miao, P.-Y. Lin, C.-T. Chen, J.-H. Juang and H.-W. Sung, *ACS Nano*, 2018, **12**, 6389–6397; (d) A. Beloqui, R. Coco, P. B. Memvanga, B. Ucar, A. Rieux and V. Pr eat, *Int. J. Pharm.*, 2014, **473**, 203–212; (e) S. Hua, E. Marks, J. J. Schneider and S. Keely, *Nanomedicine*, 2015, **11**, 1117–1132.
- C. T. H. Nguyen, R. I. Webb, L. K. Lambert, E. Stroumina, E. C. Lee, M.-O. Parat, M. A. McGuckin, A. Popat, P. J. Cabot and B. P. Ross, *ACS Appl. Mater. Interfaces*, 2017, **9**, 9470–9483.
- S. Merouani, O. Hamdaoui, F. Saoudi and M. Chiha, *Chem. Eng. J.*, 2010, **158**, 550–557.
- L. D. Freedman and G. O. Doak, *Chem. Rev.*, 1957, **57**, 479–523.